Electronic Supplementary Material (ESI) for Journal of Materials Chemistry C.

Supporting Information

Non-doped organic light-emitting diodes based on phenanthroimidazole-triphenylamine derivatives with a low efficiency roll-o□ of 9% at a high luminance of 10000 cd m^{-2}

Chunya Du, Futong Liu, Hui Liu, Xin He, Dongyan Jiang, Zijun Feng, Lei Gao, and Ping Lu*

State Key Laboratory of Supramolecular Structure and Materials, Department of Chemistry, Jilin University, Qianjin Street No. 2699, Changchun, 130012, P. R. China

*Corresponding authors:

E-mail: lup@jlu.edu.cn

Table of Contents

1. Experimental Section

General Information

All the reagents and solvents used for the synthesis and characterization were purchased and used without further purification. The ^{1}H NMR data were recorded on a Bruker AVANCE 500 spectrometer at 500 MHz, using tetramethylsilane (TMS) as the internal standard. The MALDI-TOF-MS mass spectra were measured using an AXIMA-CFRTM plus instrument. Thermal gravimetric analysis (TGA) was measured on a Perkin-Elmer thermal analysis system from 30 °C to 900 °C at a heating rate of 10 K/min under nitrogen flow rate of 80 mL/min. Differential scanning calorimetry (DSC) was performed on a NETZSCH (DSC-204) unit from 50 °C to 360 °C at a heating rate of 10 K/min under nitrogen atmosphere. The electrochemical properties (oxidation and reduction potentials) were carried out via cyclic voltammetry (CV) measurements by using a standard one-compartment, three-electrode electro-chemical cell given by a BAS 100B/W electrochemical analyzer. Tetrabutylammonium-hexafluorophosphate ($TBAPF_6$) in anhydrous dimethylformamide (DMF) or anhydrous dichloromethane (0.1 M) were used as the electrolyte for negative or positive scan. A glass-carbon disk electrode was used as the working electrode, a Pt wire as the counter electrode, Ag/Ag^+ as the reference electrode together with ferrocene as the internal standard at the scan rate of 50 mV/s. The HOMO/LUMO levels were calculated according to the following formalism:

$$E_{HOMO} = -(E_{OX} \text{ vs. } Fc/Fc^+ + 4.8)\ eV$$

$$E_{LUMO} = -(E_{red} \text{ vs. } Fc/Fc^+ + 4.8)\ eV$$

UV-vis, fluorescence spectra and PLQY (Φ_F) were recorded on a Shimadzu UV-3100 spectrophotometer using 1 cm path length quartz cells. The fluorescence lifetimes were measured by FLS920 Spectrometer. The Φ_F of different solutions were determined by using 0.1 M quinine sulfate as a reference ($\Phi_F = 0.546$) and were calculated by using the following formula:

$$Q_x = Q_r\left(\frac{A_r(\lambda_r)}{A_x(\lambda_x)}\right)\left(\frac{I(\lambda_r)}{I(\lambda_x)}\right)\left(\frac{n_x^2}{n_r^2}\right)\left(\frac{D_x}{D_r}\right)$$

Where Q is the PLQY, A is the value of absorbance, I is the intensity of excitation source, n is the refractive index of solvent, D is the area of emission spectra, λ is the corresponding wavelength.

The subscript r stands for the reference while x stands for test subject. The excitation wavelength was 375 nm and 380 nm for TPPI-BZPCN and TPPI-AQ respectively.

Device Fabrication

ITO coated glass was used as the substrate and the sheet resistance was 20 Ω square^{-1}. The ITO glass substrates were cleaned with isopropanol, alcohol, acetone, toluene and deionized water, dried in an oven at 120 °C, treated with UV-zone for 20 min, and finally transferred to a vacuum deposition system with a base pressure lower than 5×10^{-6} mbar for organic and metal deposition. The hole injecting HAT-CN layer (6 nm) was deposited at a rate of 0.1 Å s^{-1}. The deposition rate of all organic layers was 1.0 Å s^{-1}. The cathode LiF (1 nm) was deposited at a rate of 0.1 Å s^{-1} and then the capping Al metal layer (100 nm) was deposited at a rate of 4.0 Å s^{-1}. The electroluminescent (EL) characteristics were measured using a Keithley 2400 programmable electrometer and a PR-650 Spectro scan spectrometer under ambient condition at room temperature.

Computational Details

The ground state (S_0) and excited state (S_1) geometries were optimized at the B3LYP/6-31G (d, p) level. The HOMO/LUMO distributions were calculated on the basis of optimized S_0 state. The higher absorption and emission energy levels of both singlet and triplet states were calculated using B3LYP/6-31G (d, p) method on the basis of the optimized configuration of S_1, respectively. Natural transition orbitals (NTOs) of emission were evaluated for the ten lowest excited-states, involving both singlet and triplet states under B3LYP/6-31G (d, p) level.

Lippert-Mataga calculation

$$hc(\nu_a - \nu_f) = hc(\nu_a^0 - \nu_f^0) - \frac{2(\mu_e - \mu_g)^2}{a^3} f(\varepsilon, n)$$

f is the orientational polarizability of the solvent, corresponds to the Stokes shifts when f is zero, μ_e is the excited state dipole moment, μ_g is the ground-state dipole moment; a is the solvent cavity (Onsager) radius, derived from the Avogadro number (N), molecular weight (M), and density (d = 1.0 g/cm^3); ε and n are the solvent dielectric and the solvent refractive index, respectively; a and f (ε, n) can be calculated respectively as follows:

$$f(\varepsilon,n) = \frac{\varepsilon - 1}{2\varepsilon + 1} - \frac{n^2 - 1}{2n^2 + 1}$$

$$a = (3M/4N\pi l)^{1/3}$$

The detailed data are listed in **Table S1**. The stokes shift $(\nu_a - \nu_f)$ of TPPI-BZPCN and TPPI-AQ are in linear relationship with the solvent polarity f as presented in **Fig. S11**.

2. Synthesis Process

BrBZPCN

4,7-Dibromobenzo[c] [1, 2, 5] thiadiazole (4.41 g, 15 mmol), (4-cyanophenyl) boronic acid (2.30 g, 10 mmol), $Pd(PPh_3)_4$ (0.30 mmol, 0.30 g), K_2CO_3 (6.00 g, 40 mmol), distilled water (20 mL), and toluene (40 mL) were first mixed. The mixture was heated and refluxed at 90 °C under a nitrogen atmosphere for 36 h. After cooling to room temperature, the mixture was washed by water and extracted with dichloromethane consecutively. The product was then further dried with $MgSO_4$ and purified by column chromatography on silica gel using a petroleum ether/dichloromethane mixture (4:1) as the eluent. ^{1}H NMR (500 MHz, DMSO-D_6) δ (ppm): 8.23 - 8.15 (m, 3H), 8.04 (d, J = 8.5 Hz, 2H), 7.91 (d, J = 7.6 Hz, 1H). MS (MALDI-TOF), m/z: [M^+] Calcd for $C_{13}H_6BrN_3S$, 316.68; Found, 316.18.

TPA-NO_2

1-Fluoro-4-nitrobenzene (8.40 g, 60 mmol), diphenylamine (8.45 g, 50 mmol), caesium fluoride (15.21 g, 0.10 mol) and dimethyl sulfoxide (120 mL) were added and refluxed at 140 °C under N_2 atmosphere for 6 h. After the reaction, the mixture was poured into water and cooled by ice. And then, it was filtered and an orange solid was obtained. The solid was recrystallized in ethanol twice and dried to obtain the product without any further purification. MS (MALDI-TOF), m/z: [M^+] Calcd for $C_{18}H_{16}N_2O_2$, 290.32; Found, 290.80

TPA-NH_2

TPA-NO_2 (5.86 g, 20 mmol), $SnCl_2 \cdot 2H_2O$ (27.05 g, 120 mmol), and ethyl alcohol (120 mL) were mixed and refluxed at 70 °C under N_2 atmosphere for 100 min. After cooling to room temperature, the mixture was quenched by sodium hydroxide solution and extracted with dichloromethane consecutively. Afterwards, the dichloromethane was removed by distillation and get the product, without any further purification. MS (MALDI-TOF), m/z: [M^+] Calcd for $C_{18}H_{16}N_2$, 260.34; Found, 260.43

TPPIBr

TPPIBr was synthesized in a one-pot reaction. The mixtures of phenanthrenequinone (2.10 g, 10 mmol), TPA-NH_2 (10.00 g, 40 mmol), ammonium acetate (4.01 g, 50 mmol), 4-bromobenzaldehyde (1.85 g, 10 mmol) and acetic acid (50 mL) were reacted in acetic acid at 120 °C under N_2 atmosphere for 2 h. After the reaction, the mixture was poured into water and cooled by ice. And then, it was filtered and the crude product was obtained, washed with acetic acid, water, and ethyl alcohol in turn, then purified through chromatography to give TPPIBr as light-yellow powder with good yield. ^{1}H NMR (500 MHz, DMSO-D_6) δ (ppm): 8.95 (d, J = 8.3 Hz, 1H), 8.89 (d, J = 8.2 Hz, 1H), 8.68 (d, J = 7.1 Hz, 1H), 7.77 (d, J = 7.1 Hz, 1H), 7.72 - 7.66 (m, 3H), 7.62 (t, J = 8.1 Hz, 3H), 7.53 (dd, J = 16.3, 8.4 Hz, 3H), 7.48-7.40 (m, 4H), 7.38 (d, J = 7.7 Hz, 1H), 7.23 (d, J = 7.6 Hz, 4H), 7.20 - 7.12 (m, 4H). MS (MALDI-TOF), m/z: [M^+] Calcd for $C_{39}H_{26}BrN_3$, 616.56; Found, 616.43.

TPPIB

KOAc (1.50 g, 15 mmol), PPIBr (3.00 g, 5 mmol), bis(pinacolato)diboron (2.53 g, 10 mmol), Pd(dppf)Cl_2 (0.12 g, 0.15 mmol) and dioxane (30 mL) were first mixed. The mixture was heated by 90 °C and refluxed under a nitrogen atmosphere for 48 h. After cooling to room temperature, the mixture was washed by water and extracted with dichloromethane consecutively. The dichloromethane was removed by distillation. The product was then further dried with $MgSO_4$ and purified by column chromatography on silica gel using a petroleum ether/ dichloromethane mixture (1:2) as the eluent, and the pure product of TPPIB was finally obtained. ^{1}H NMR (500 MHz, DMSO-D_6) δ (ppm): 8.95 (d, J = 8.2 Hz, 1H), 8.89 (d, J = 8.4 Hz, 1H), 8.69 (d, J = 6.8 Hz, 1H), 7.77 (t, J = 7.5 Hz, 1H), 7.71 (dt, J = 8.3, 7.3 Hz, 5H), 7.62 (t, J = 7.7 Hz, 1H), 7.53 (dd, J = 12.0, 5.3 Hz, 3H), 7.42 (dd, J = 17.2, 9.7 Hz, 4H), 7.39 (d, J = 7.6 Hz, 1H), 7.22 (d, J = 7.6 Hz, 4H), 7.20 - 7.11 (m, 4H), 1.34 (s, 12H). MS (MALDI-TOF), m/z: [M^+] Calcd for $C_{45}H_{38}BN_3O_2$, 663.63; Found, 663.81.

TPPI-AQ

TPPIB (3.31 g, 5 mmol), 2-bromoanthracene-9,10-dione (1.72 g, 6 mmol), Pd(PPh_3)$_4$ (0.15 g, 0.15 mmol), K_2CO_3 (6.00 g, 40 mmol), distilled water (20 mL), and toluene (40 mL) were first mixed. The mixture was heated by 90 °C and refluxed under a nitrogen atmosphere for 36 h. After cooling to room temperature, the mixture was washed by water and extracted with dichloromethane consecutively. The product was then further dried with $MgSO_4$ and purified by column

chromatography on silica gel using a petroleum ether/dichloromethane mixture as the eluent to obtain pure product of TPPI-AQ. ^{1}H NMR (500 MHz, DMSO-D_6) δ (ppm): 9.58 (dd, *J* = 11.7, 8.2 Hz, 2H), 9.51 (d, *J* = 7.6 Hz, 1H), 8.49 (d, *J* = 7.8 Hz, 2H), 8.48 - 8.41 (m, 2H), 8.36 - 8.32 (m, 1H), 8.26 (d, *J* = 9.8 Hz, 2H), 8.20 (dd, *J* = 19.9, 7.2 Hz, 3H), 8.05 (dd, *J* = 15.3, 8.9 Hz, 2H), 7.97 (s, 3H), 7.62 (d, *J* = 8.5 Hz, 2H), 7.58-7.54 (m, 1H), 7.46-7.35 (m, 5H), 7.21 (dd, *J* = 9.9, 7.5 Hz, 4H), 7.16-7.11 (m, 2H), 7.08 (d, *J* = 7.3 Hz, 1H). ^{13}C NMR (126 MHz, $CDCl_3$) δ (ppm): 183.48, 148.14, 147.71, 147.46, 145.86, 143.67, 143.17, 142.36, 141.89-141.05, 134.37, 131.71, 131.43, 130.98, 129.99, 129.84, 129.82, 129.09, 128.35, 128.35, 127.08, 126.99,126.50, 126.31, 125.17, 124.81, 124.81,124.06, 124.14, 123.49, 123.17, 122.45. MS (MALDI-TOF), m/z: [M^+] Calcd for $C_{53}H_{33}N_3O_2$, 743.26; Found, 743.81. Elem. Anal. Calcd for $C_{53}H_{33}N_3O_2$: C, 85.58; H, 4.47; N, 5.65. Found: C, 85.40; H, 4.45; N, 5.54.

TPPI-BZPCN

TPPIB (3.30 g,5 mmol), BrBZPCN (1.92 g, 6 mmol), Pd (PPh_3)$_4$ (0.15 g, 0.15 mmol), K_2CO_3 (6.00 g, 40 mmol), distilled water (20 mL), and toluene (40 mL) were first mixed. The mixture was heated by 90 °C and refluxed under a nitrogen atmosphere for 36 h. After cooling to room temperature, the mixture was washed by water and extracted with dichloromethane consecutively. The product was then further dried with $MgSO_4$ and purified by column chromatography on silica gel using a petroleum ether/dichloromethane mixture as the eluent to obtain pure product of TPPI-BZPCN. ^{1}H NMR (500 MHz, DMSO-D_6) δ (ppm): 8.97 (d, *J* = 8.3 Hz, 1H), 8.91 (d, *J* = 8.5 Hz, 1H), 8.73 (d, *J* = 8.0 Hz, 1H), 8.28 (d, *J* = 8.3 Hz, 2H), 8.14 (dt, *J* = 15.8, 7.9 Hz, 4H), 8.07 (d, *J* = 8.4 Hz, 2H), 7.89 (d, *J* = 8.4 Hz, 2H), 7.82-7.78 (m, 1H), 7.71 (t, *J* = 7.0 Hz, 1H), 7.63 (d, *J* = 8.7 Hz, 3H), 7.56-7.52 (m, 1H), 7.42 (dd, *J* = 13.8, 6.3 Hz, 5H), 7.28-7.18 (m, 6H), 7.17 (t, *J* = 7.4 Hz, 2H). ^{13}C NMR (126 MHz, $CDCl_3$) δ (ppm): 153.91, 153.65, 150.33, 149.19, 147.02, 141.69, 137.29, 137.13-136.79, 132.39, 131.41, 130.92, 130.27, 129.09, 128.83, 128.77,127.88, 127.96, 127.96, 127.27, 126.32, 125.69, 125.28, 125.01, 124.14, 123.06, 122.77, 121.00, 118.82. MS (MALDI-TOF), m/z: [M^+] Calcd for $C_{52}H_{32}N_6S$, 772.24; Found, 772.81. Elem. Anal. Calcd for $C_{52}H_{32}N_6S$: C, 80.81; H, 4.17; N, 10.87. Found: C, 80.56; H, 4.32; N, 10.19.

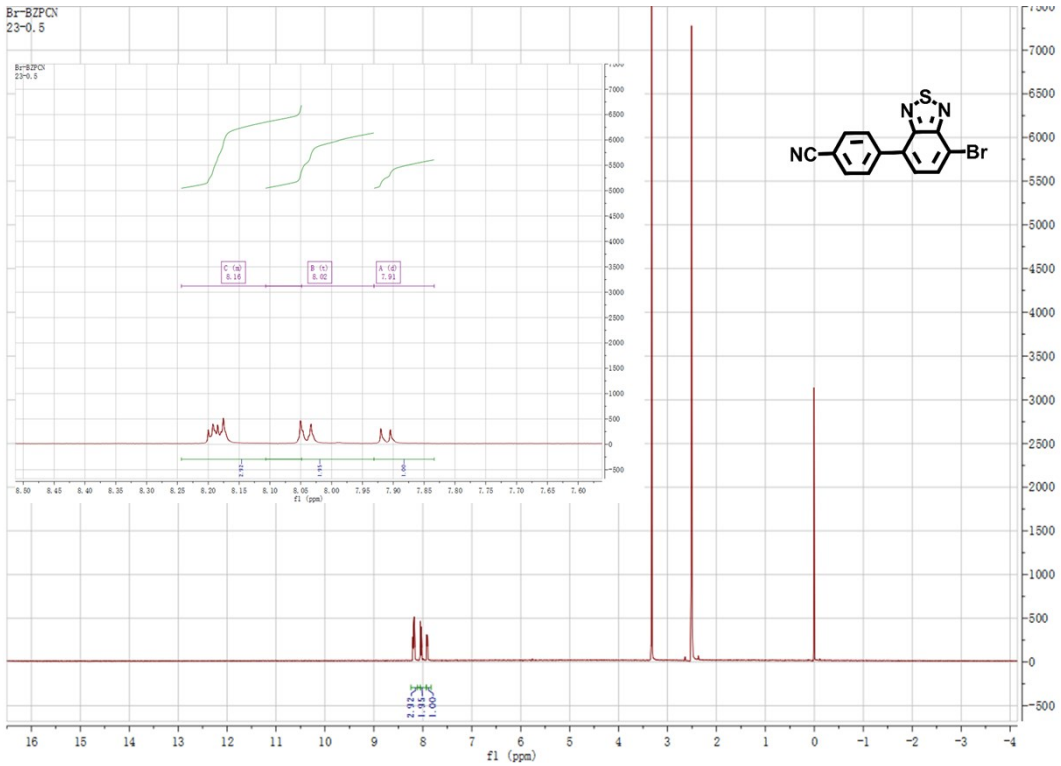

Fig. S1 ^{1}H NMR spectrums of BZPCNBr measured in deuterated DMSO-D_6.

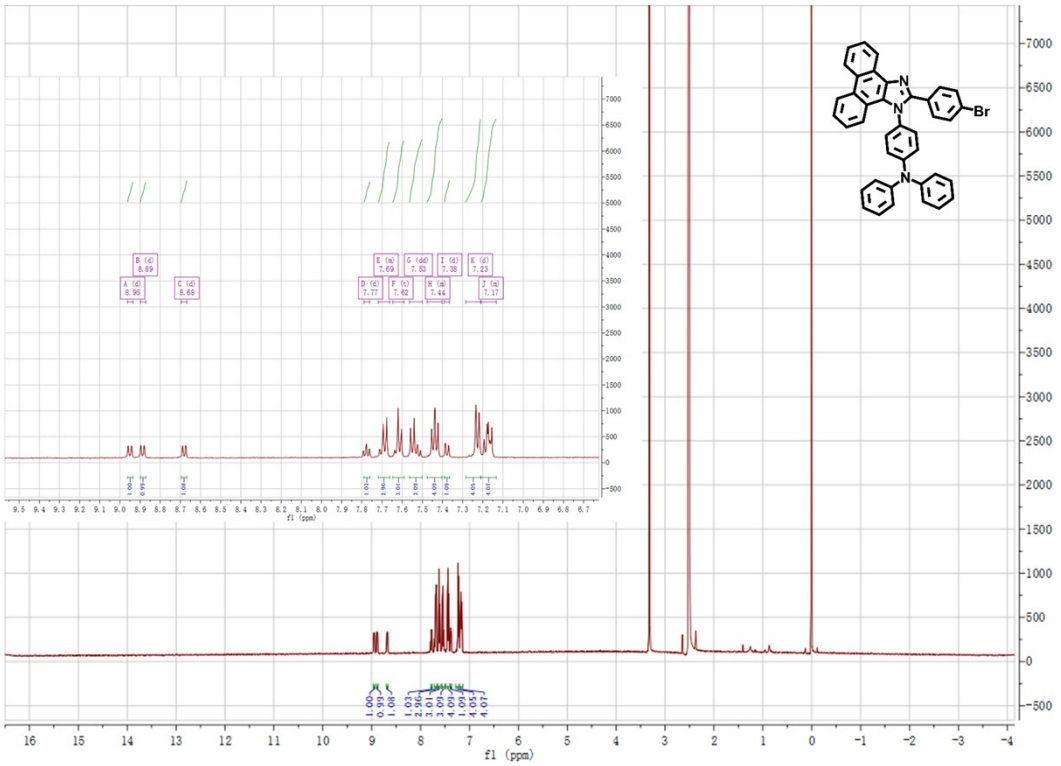

Fig. S2 ^{1}H NMR spectrums of TPPIBr measured in deuterated DMSO-D_6.

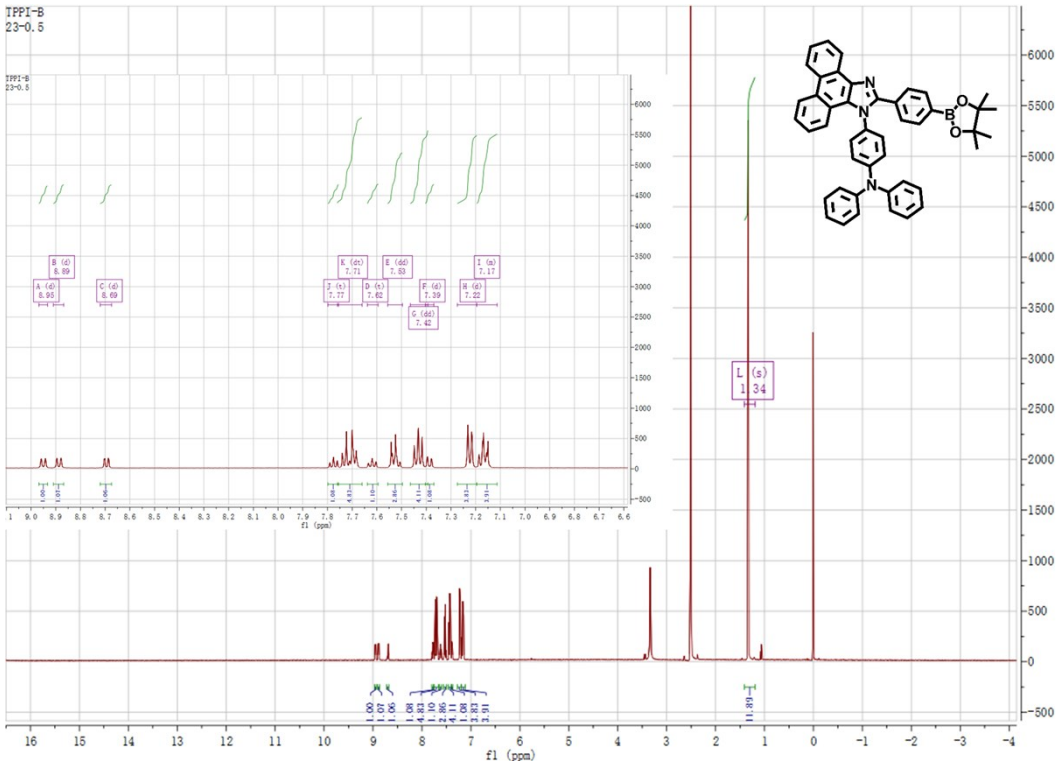

Fig. S3 ^{1}H NMR spectrums of TPPIB measured in deuterated DMSO-D_6.

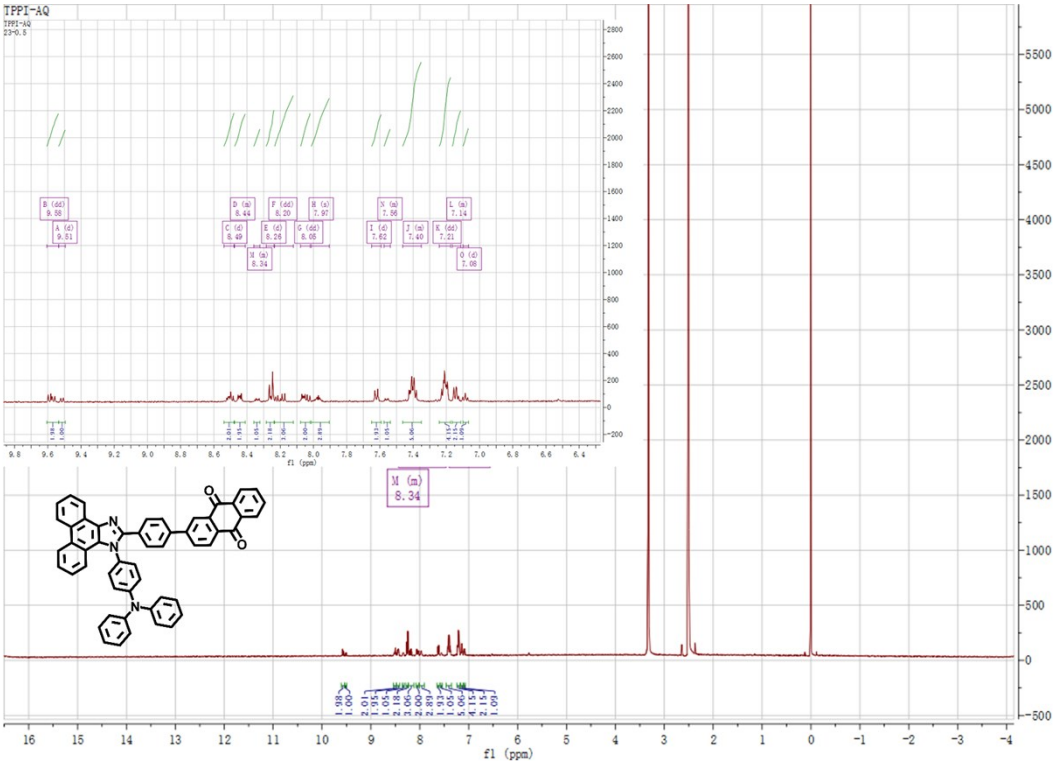

Fig. S4 ^{1}H NMR spectrums of TPPI-AQ measured in deuterated DMSO-D_6.

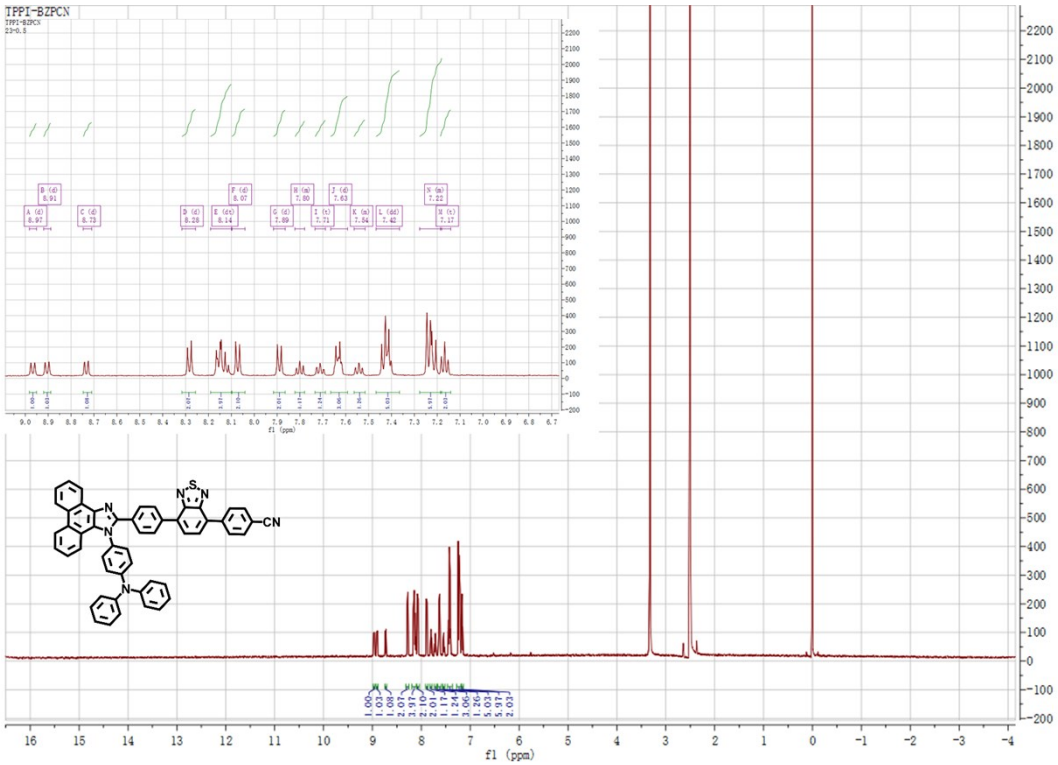

Fig. S5 ^{1}H NMR spectrums of TPPI-BZPCN measured in deuterated DMSO-D_6.

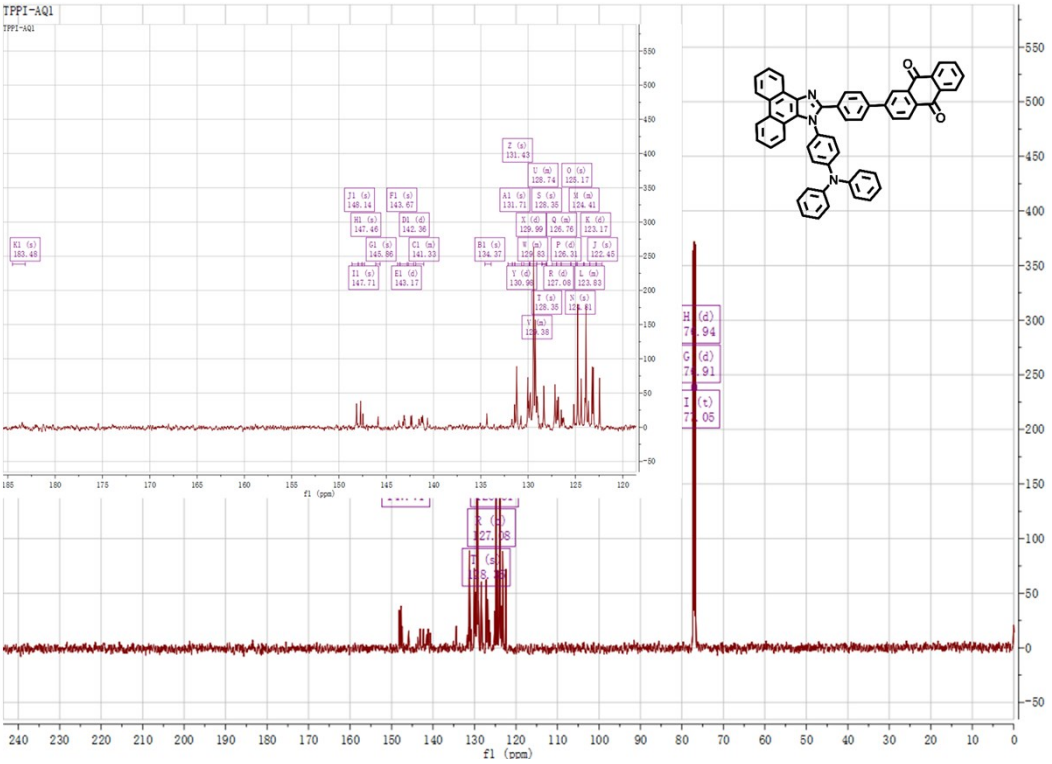

Fig. S6 ^{13}C NMR spectrums of TPPI-AQ measured in deuterated CD_2Cl_2.

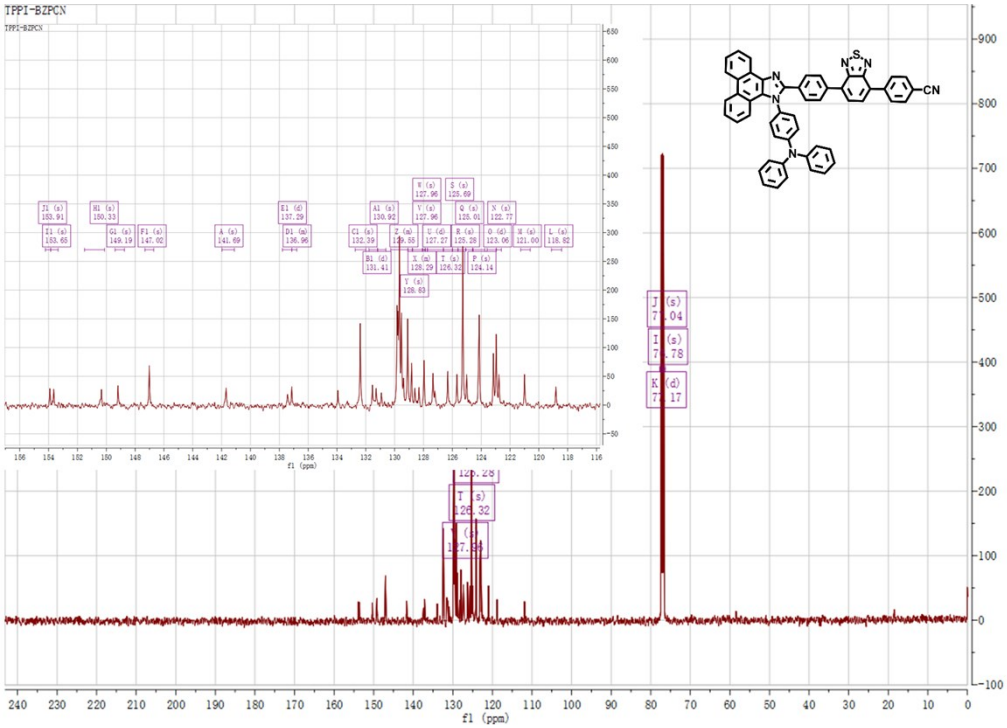

Fig. S7 ^{13}C NMR spectrums of TPPI-BZPCN measured in deuterated CD_2Cl_2.

3. Photophysical Properties

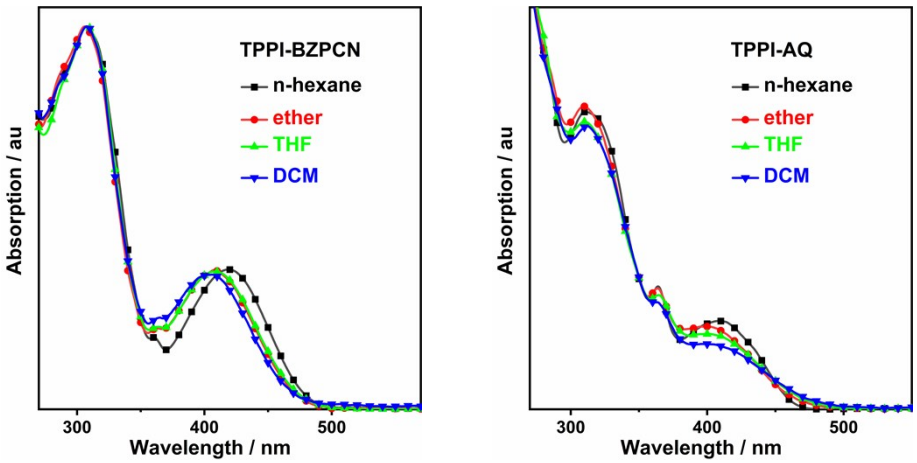

Fig. S8 Solvation effects on UV/vis absorption of TPPI-BZPCN and TPPI-AQ.

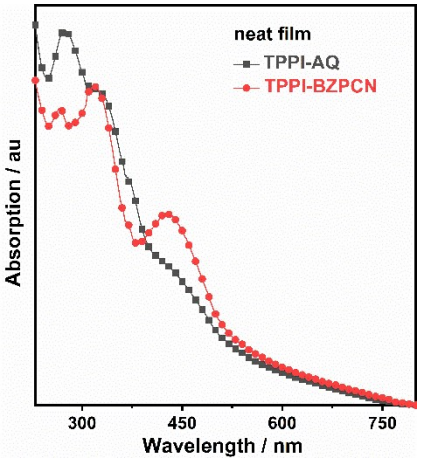

Fig. S9 Absorption of TPPI-BZPCN and TPPI-AQ neat film.

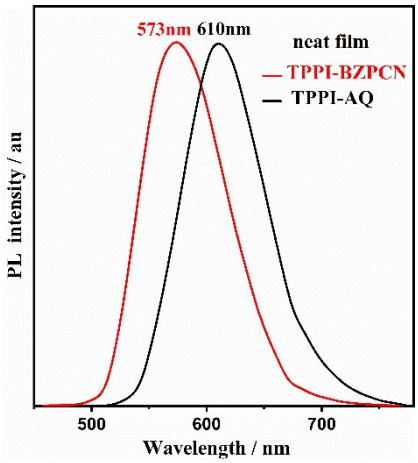

Fig. S10 PL spectra of TPPI-BZPCN and TPPI-AQ in vacuum evaporated film.

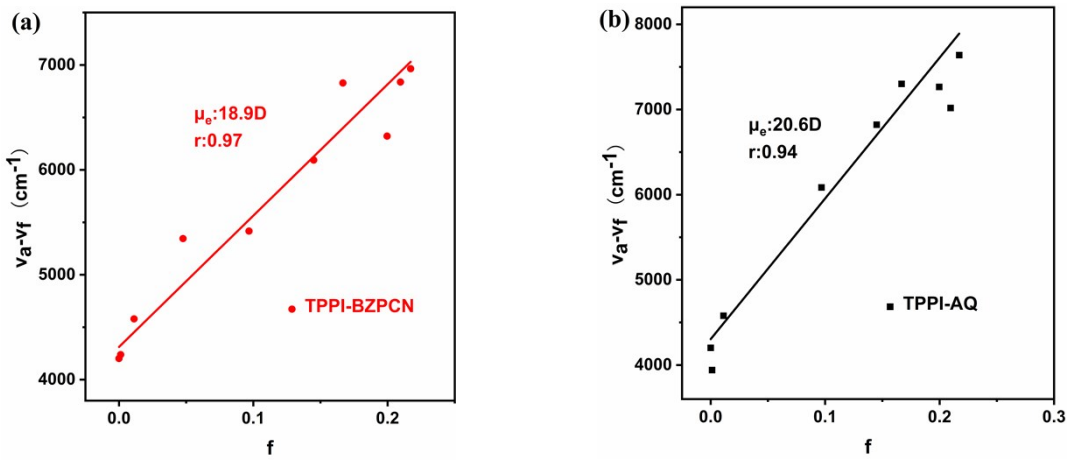

Fig. S11 Linear correlation of orientation polarization (f) of solvent media with the stokes shift (ν_a-ν_f); a: absorbed light; f: fluorescence for TPPI-BZPCN (a) and TPPI-AQ (b) (**Table S1** for the solvents and corresponding data).

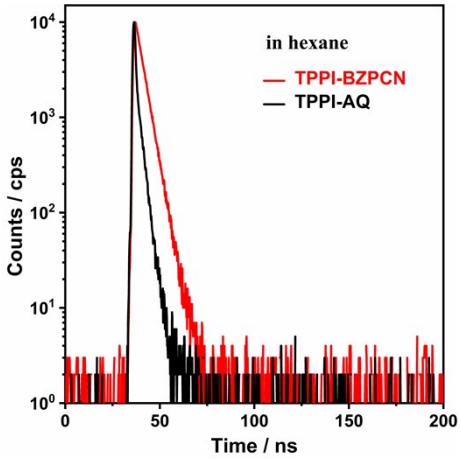

Fig. S12 Transient photoluminescence decay measurement of TPPI-BZPCN and TPPI-AQ in hexane solution.

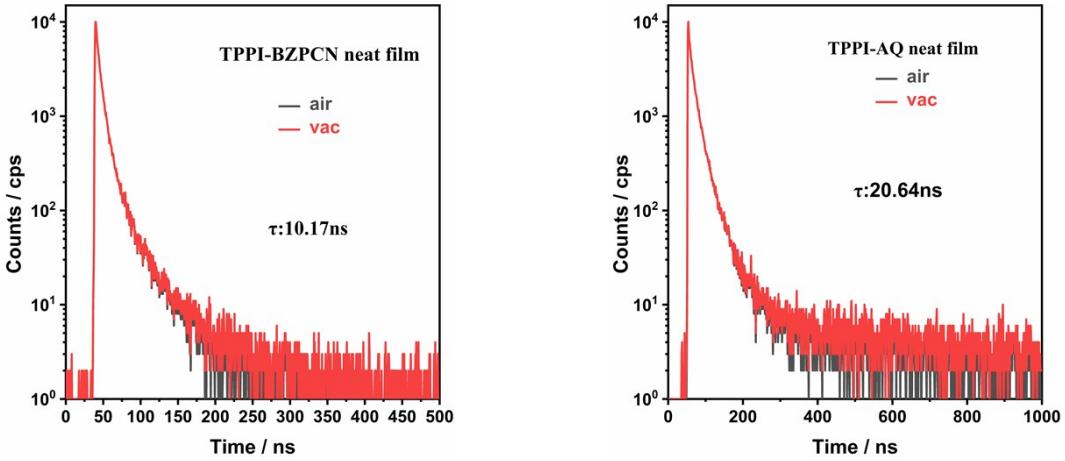

Fig. S13 Transient photoluminescence decay measurement of TPPI-BZPCN and TPPI-AQ in neat film under air and degassed condition.

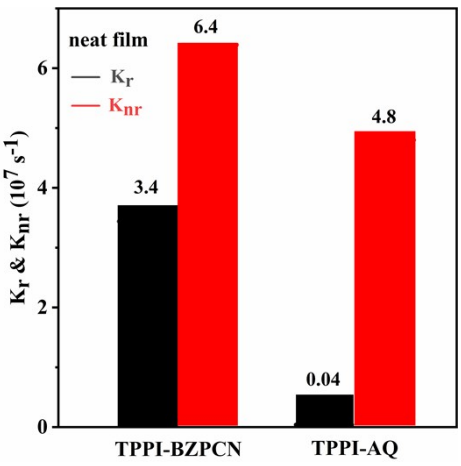

Fig. S14 Radiative transition rates (k_r) and non-radiative transition rates (k_{nr}) of TPPI-BZPCN and TPPI-AQ in neat film.

Table S1 Detailed photophysical data of TPPI-BZPCN and TPPI-AQ in different solvents.

Solvents	f (ε, n)	Φ_F	TPPI-BZPCN		
			λ_{abs} (nm)	λ_{em} (nm)	ν_a-ν_f (cm^{-1})
Hexane	~ 0	0.50	418	508	4238
Cyclohexane	~ 0	0.39	420	510	4202
Tetrachloromethane	0.011	0.40	420	520	4579
Triethylamine	0.048	0.38	416	530	5345
Butyl ether	0.096	0.34	408	537	5416
Isopropyl ether	0.145	0.30	407	543	6093
Ethyl ether	0.167	0.32	405	548	6828
Ethyl acetate	0.200	0.06	410	556	6321
Tetrahydrofuran	0.210	0.06	405	562	6836
Methylene chloride	0.217	0.05	410	568	6964
Dimethyl formamide	0.276	~ 0	405	n.d	--
Acetone	0.284	~ 0	404	n.d	--
Acetonitrile	0.305	~ 0	395	n.d	--

Solvents	f (ε, n)	Φ_F	TPPI-AQ		
			λ_{abs} (nm)	λ_{em} (nm)	ν_a-ν_f (cm^{-1})
Hexane	~ 0	0.05	410	489	3940
Cyclohexane	~ 0	0.04	412	485	3653
Tetrachloromethane	0.011	0.03	412	522	5114
Triethylamine	0.048	0.02	406	543	6275
Butyl ether	0.096	0.02	407	541	6085
Isopropyl ether	0.145	0.03	403	552	6821
Ethyl ether	0.167	~ 0	400	553	7300
Ethyl acetate	0.200	~ 0	405	552	7264
Tetrahydrofuran	0.210	~ 0	406	560	7018
Methylene chloride	0.217	~ 0	409	576	7638
Dimethyl formamide	0.276	~ 0	397	n.d	--
Acetone	0.284	~ 0	399	n.d	--
Acetonitrile	0.305	~ 0	401	n.d	--

λ_{abs}: absorption maximum; λ_{em}: emission maximum; Φ_F: fluorescence quantum yield estimated by using quinoline sulfate as standard (Φ_F = 54.6% in 0.1 M sulfuric acid solution), and n.d = not detectable (signal too weak to be accurately determined).

4. Theoretical Calculations

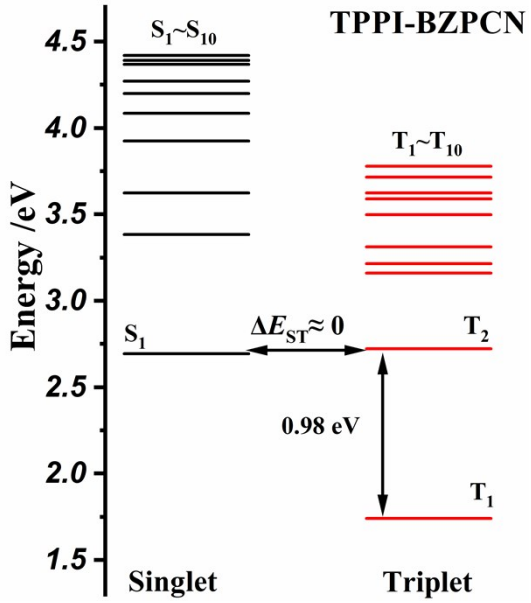

Fig. S15 Excited state (singlet and triplet) energy diagram of TPPI-BZPCN at the geometry of S_1 state.

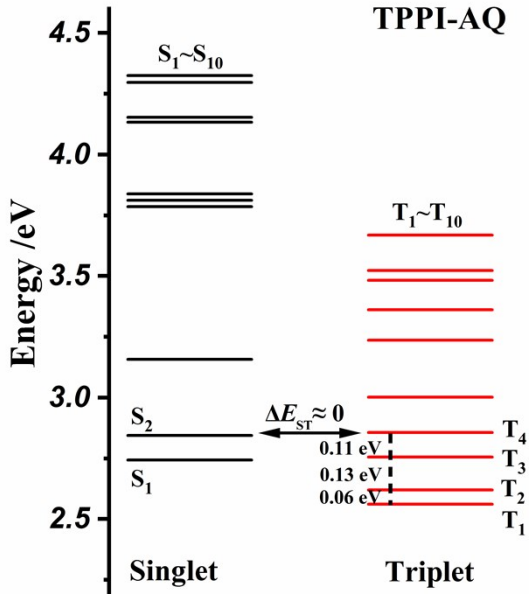

Fig. S16 Excited state (singlet and triplet) energy diagram of TPPI-AQ at the geometry of S_1 state.

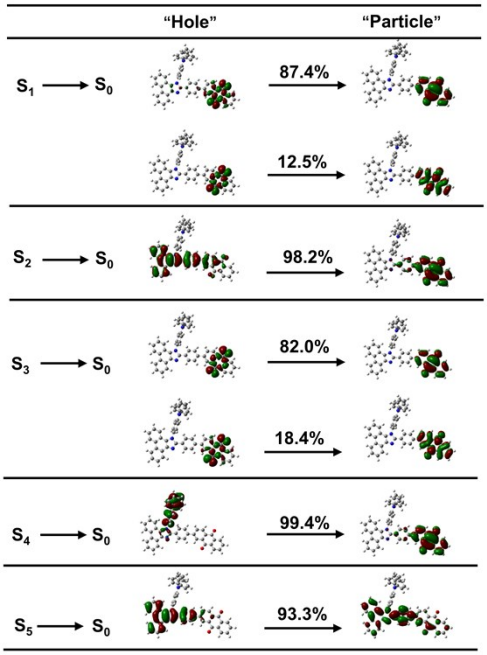

Fig. S17 Natural transition orbitals of TPPI-AQ singlet excited states (S_1 to S_5).

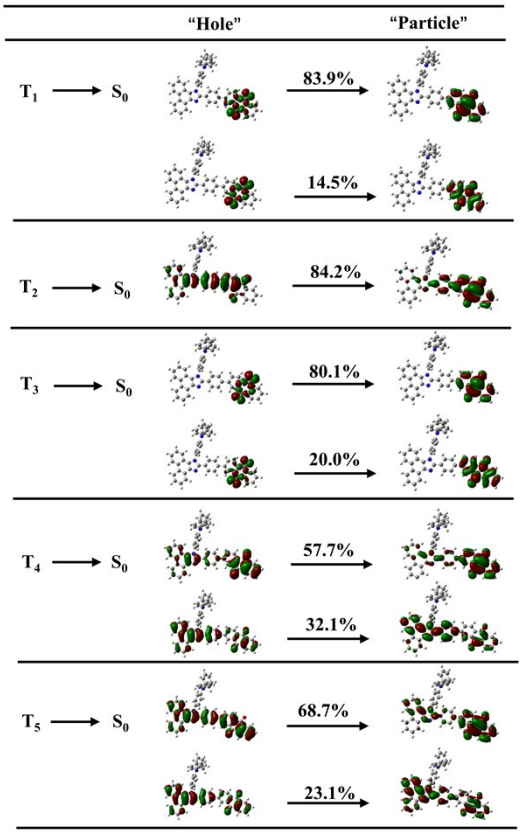

Fig. S18 Natural transition orbitals of TPPI-AQ triplet excited states (T_1 to T_5).

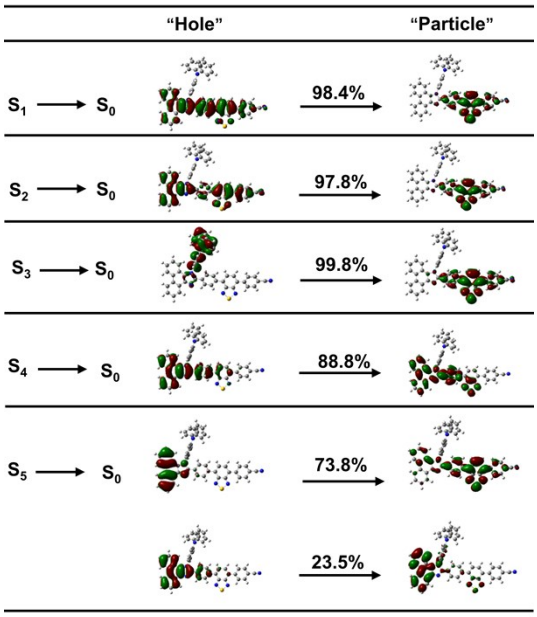

Fig. S19 Natural transition orbitals of TPPI-BZPCN singlet excited states (S_1 to S_5).

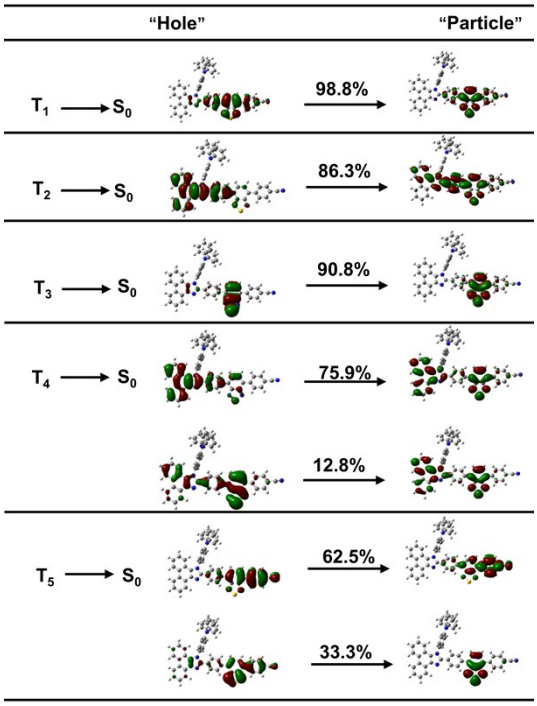

Fig. S20 Natural transition orbitals of TPPI-BZPCN triplet excited states (T_1 to T_5).

Table S2 Energy level, singlet and triplet states of TPPI-BZPCN and TPPI-AQ.

Excited States	TPPI-BZPCN		TPPI-AQ	
	S (eV)	T (eV)	S (eV)	T (eV)
1	2.6930	1.7395	2.7440	2.5612
2	3.3842	2.7222	2.8445	2.6204
3	3.6229	3.1591	3.1579	2.7549
4	3.9243	3.2159	3.7855	2.8571
5	4.0856	3.3129	3.8113	3.0014

5. Electroluminescence Property

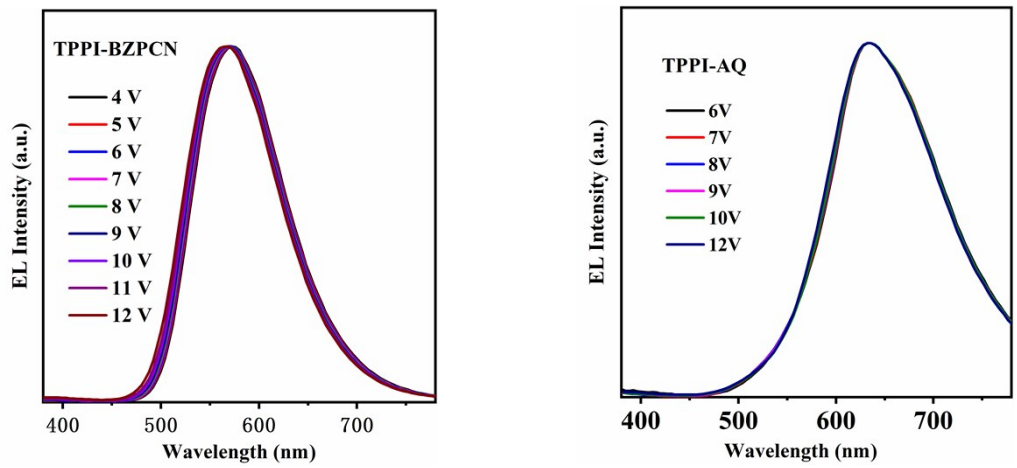

Fig. S21 Normalized EL spectra of non-doped devices based on TPPI-BZPCN and TPPI-AQ at different voltages.

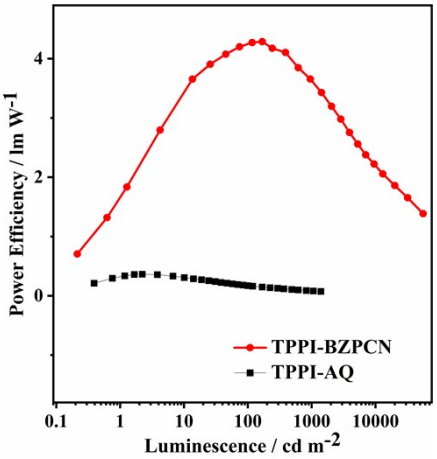

Fig. S22 Power efficiencies versus luminance curves of non-doped devices based on TPPI-BZPCN and TPPI-AQ.